ISSN 1062-7391, Journal of Mining Science, 2021, Vol. 57, No. 1, pp. 154–170. © Pleiades Publishing, Ltd., 2021.
Russian Text © The Author(s), 2021, published in Fiziko-Tekhnicheskie Problemy Razrabotki Poleznykh Iskopaemykh, 2021, No. 1, pp. 169–188.

MINING

THERMOPHYSICS

The Analysis of Thermal Conditions in Extra-Long Railway Tunnels during the Cold Season

L. A. Kiyanitsa[a], I. V. Lugin[a], and A. M. Krasyuk[a,b]*

[a]*Chinakal Institute of Mining, Siberian Branch, Russian Academy of Sciences, Novosibirsk, 630091 Russia*
**e-mail: kkrasuk@cn.ru*
[b]*Novosibirsk State Technical University, Novosibirsk, 630073 Russia*

Received November 5, 2020
Revised December 10, 2020
Accepted January 15, 2021

Abstract—The subcool zone length is determined in lining of an extra-long railway tunnel subjected to deep influence of piston effect. The air temperature distribution in the outer air–tunnel lining contact zone is determined as function of the velocity of train and the outdoor temperature in the cold season. The authors review the de-icing methods of tunnel lining: warming-up using a self-tuning heating cable; arrangement of an unheated access gallery and heat insulation. The distribution of the hourly average air temperature in an extra-long railway tunnel is analyzed against of sites of fan heaters. The heat power patterns in the tunnel are estimated by the criterion of the required temperature conditions. It is shown that the most efficient arrangement of fan heaters to maintain the required air temperature in the tunnel is their uniform distribution along the length of the tunnel in combination with installation of warm air curtains at the tunnel faces.

Keywords: Railway tunnel, ventilation, heat exchange, temperature distribution, fan heater, cool gallery, heating cable, energy efficiency criterion.

DOI: 10.1134/S1062739121010166

INTRODUCTION

In Russian Siberia and Far East, cargo carriage is mainly performed by railway. Reliability and uninterrupted operation of railway infrastructure, including railway tunnels, are very critical in this regard. The mentioned regions are specific for low temperatures in the cold seasons and for difficult geological conditions, in particular, high water content of enclosing rock mass surrounding the tunnels. The service experience shows that air temperature in the operating tunnels in the cold seasons is below standard [1, 2] specified in the effective regulations [3], which calls for the updating of the thermal environment design procedures and necessitates additional studies into the temperature variation patterns in railway tunnels.

1. SUBCOOL EXTENSION AND TEMPERATURE DISTRIBUTION IN THE TUNNEL FACE AREAS

In the cold seasons, the operating tunnels of the Baikal–Amur Mainline are generally faced with frosting and icing of rails and lining in the areas at tunnel faces equipped with closable gates [1]. Due to the cyclical effect of the outdoor temperatures, tunnel lining is exposed to continuous free–thaw, which promotes rapid frost destruction. Cold outside air enters the tunnel together with trains as there is a zone of negative static pressure behind the train tail car. Every time as a train leaves the tunnel, via the train and tunnel clearance, much outside air comes into the tunnel in the amount comparable with the volume of the train.

For validating the lining de-frost control at the outlet face of a tunnel, it is required to determine:

—the length of the subcool zone in the lining from the outlet face depthward the tunnel;

—the inside air temperature distribution from the outlet face depthward the tunnel depending on the technological parameters of the tunnel and its climate.

The experiments were implemented using the computational aerodynamics and heat exchange methods (control volume approach) in Ansys CFX. The equations below were solve using the RNG $k-\varepsilon$ turbulence model:

Equation of continuity

$$\frac{\partial \rho}{\partial \tau}+\nabla(\rho\vec{u})=0, \tag{1}$$

Momentum conservation equation

$$\frac{\partial(\rho\vec{u})}{\partial \tau}+\nabla(\rho\vec{u}\otimes\vec{u})=-\nabla p+\nabla\Lambda+S_M, \tag{2}$$

Energy equation

$$\frac{\partial(\rho h)}{\partial \tau}-\frac{\partial p}{\partial \tau}+\nabla(\rho\vec{u}h)=\nabla(\lambda\nabla t)+\Lambda:\nabla\vec{u}+S_E. \tag{3}$$

Here, $\Lambda=\mu[\nabla\vec{u}+(\nabla\vec{u})^{\mathrm{T}}-(2/3\delta\nabla\vec{u}]$ is the tensor of friction forces; t is the air temperature, °C; T is the index of the skew-symmetric matrix; $\vec{u}$ is the velocity vector field; τ is the time, s; ∇ is the Hamilton operator; $\otimes$ is the tensor product operator; δ is the Kronecker delta-function; μ is the dynamic viscosity, Pa·s; ρ is the density, kg/m^3; p is the pressure, Pa; λ is the heat conductivity factor, W/(m°C); h is the enthalpy, J; S_M, S_E are the point sources of impulse and energy (including heat), $\Lambda:\nabla\vec{u}$ is the dissipative energy typical of viscous fluid flows [4].

The RNG $k-\varepsilon$ model is described with the equations below:

$$\rho\frac{\partial k}{\partial \tau}+\nabla(\vec{u}k\rho)=\nabla\left(\left[\mu+\frac{\mu_t}{\sigma_k}\right]\nabla k\right)+P_k-\rho\varepsilon+P_{kb}, \tag{4}$$

$$\rho\frac{\partial \varepsilon}{\partial \tau}+\nabla(\vec{u}\varepsilon\rho)=\nabla\left(\left[\mu+\frac{\mu_t}{\sigma_{\varepsilon RNG}}\right]\nabla\varepsilon\right)+\frac{\varepsilon}{k}(C_{\varepsilon 1RNG}P_k-C_{\varepsilon 2RNG}\varepsilon\rho+C_{\varepsilon 1RNG}P_{\varepsilon b}), \tag{5}$$

$$\mu_t=C_\mu\rho\frac{k^2}{\varepsilon}, \tag{6}$$

where k is the turbulent kinetic energy, J/kg; ε is the dissipative turbulent kinetic energy, J/(kg·s); μ, μ_t are the dynamic viscosity and the turbulent dynamic viscosity, Pa·s, respectively; $\sigma_k=1$, $\sigma_{\varepsilon RNG}=0.7179$, $C_{\varepsilon 2RNG}=1.68$, $C_\mu=0.09$ are the constants of the turbulence model; P_k, P_{kb}, $C_{\varepsilon 1RNG}$, $P_{\varepsilon b}$ are the values found from the solutions of additional equations [4].

Convective heat tranfer between tunnel air and lining is set as the third-order boundary condition:

$$q_k=\alpha(t-t_s); \tag{7}$$

here, q_k is the heat flow, W/m^2; α is he heat transfer coefficient, W/(m^2·°C); t_s is the surface temperature of lining, °C.

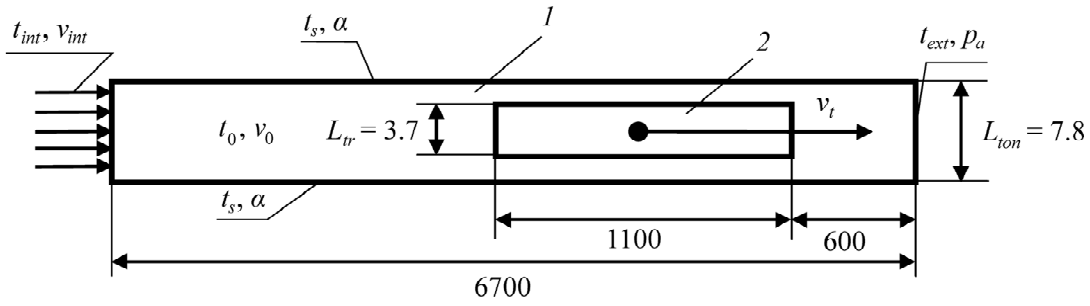

Fig. 1. Geometry and boundary conditions of heat transfer and mass exchange model at the moment of train exit from the tunnel: *1*—tunnel; *2*—train; t_0, v_0—initial temperature and velocity of air in the tunnel; t_{int}, v_{int}—temperature and velocity of air in the computation span; v_t—train velocity; t_{ext}, p_a—outer air temperature and pressure; t_s, α—natural temperature of lining and heat transfer coefficient from back of lining to tunnel air.

The geometry of the heat tranfer and mass exchange model at the moment of train exit from the tunnel as well as the boundary conditions are shown in Fig. 1. The 2D model represents a tunnel span 6700 m long with a train 1100 m long. The sizes L_{tr} and L_{ton} equal the hydraulic diameters of the tain and tunnel, respectively (3.7 and 7.8 m). The train velocity is assumed as 75 and 40 km/h. The initial conditions are: the tunnel air temperature $t_0 = 4$ °C, the air velocity $v_{int} = 0.9$ m/s, the outer air temperature in a range from –10 to –50°C. The vectors of the rain velocity v_t and air velocity v_{int} are specified in Fig. 1.

The operating conditions of the tunnel in the experiment set that gates are closed at one of the tunnel faces. The ratio of the train and tunnel cross section areas S_t and S is $S / S_t = 0.27$ (Severomuysky Tunnel) and 0.36 (Baikal Tunnel). The heat power of the fan heater installation at the outlet face is neglected in the computational experiment.

The time step $\Delta\tau = 0.1$ s is set so that the Courant criterion is under 1 at any point of the computation [5]. The subcool zone is understood as the span from the outlet face inward the tunnel along which the air temperature is never higher than 0°C.

Figure 2 offers relationships between the average air temperature and heat loss Q in warming incoming air in different cross section of the tunnel nearby the outlet face at the train velocity of 75 km and the outer air temperature $t_{ext} = -50$ C.

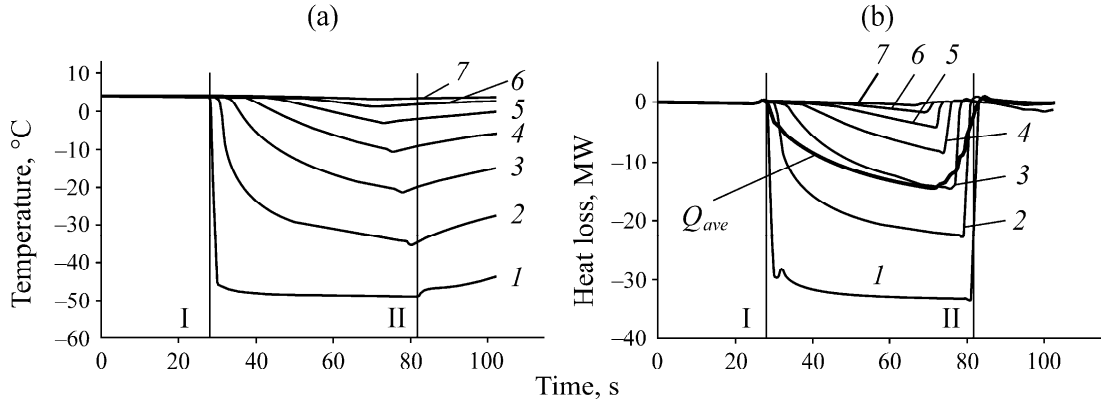

Fig. 2. (a) Air temperature and (b) heat loss in incoming air warming in different tunnel cross sections: *1*—at the outlet face; *2*—50 m away from the outlet face inward the tunnel; *3*–*7*—at the distances of 100, 150, 200, 250 and 300 m away from the outlet face inward the tunnel, respectively; Q_{ave}—average heat loss in subcool zone; I—point when the head car enters the outlet face; II—point when tail car leaves the outlet face.

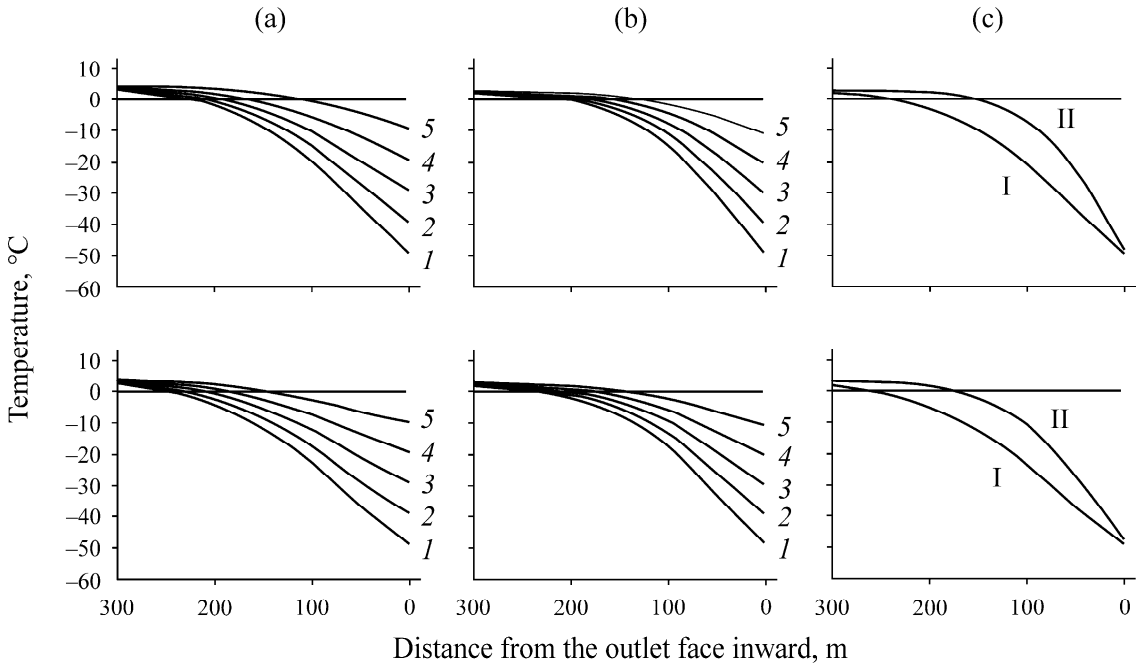

Fig. 3. Tunnel air temperature at the point of tail car exit from outlet face at the train/tunnel cross section overlap ratios of 0.27 (top curves) and 0.36 (bottom curves) in the tunnel with closed gates at the train velocities of (a) 75 and (b) 40 km/h; and (c) comparison of operating conditions in the tunnel with closable gates (I) and with open faces (II) at t_{ext} = –50°C; *1*—t_{ext} = –50°C; *2*—40; *3*—30; *4*—20; *5*—10°C.

As a train leaves the outlet face, cold atmospheric air enter the tunnel and supercooling is higher in the tunnel cross sections nearby the face (cross sections *1–7* Fig. 2). The experiment shows that at a distance of 259 m from the outlet face inward the tunnel, the tunnel air is never lower than 0°C. After the tail car leaves the tunnel, the tunnel air temperature gradually increases. The rise time of the specified temperature of 4°C in the tunnel depends on the train tail air velocity in the tunnel due to the piston effect. It is seen in Fig. 2b that the heat loss in warming the incoming outer air is very high (to 33.2 MW) but within a short time.

Figure 3 demonstrates the tunnel air temperature at the point when the tail car leaves the outlet face versus the distances to the outlet face at the train / tunnel cross section overlap ratios of 0.27 and 0.36 for the train velocities of 75 and 40 km/s. The subcool zone is within 245 m in all cases. At the higher train velocity and overlap ratio, the subcool length extends as the air velocity in the train–tunnel lining clearance increases. The outer air temperature also has influence on the extension of the subcool span: the subcool length is shorter with the higher outer air temperature.

The analytical description of the subcool span length uses the quadratic interpolation with Lagrange polynomial (Table 1, relation (8)).

Table 1. Subcool span length L_x (m) at the outlet face for the train velocities of 75 and 40 km and at the train/tunnel cross section overlap ratios of 0.27 and 0.36 in the outer air temperature range of –50 ÷ –10°C

S_t / S	v_t, km/h	t_{ext}, °C				
		–50	–40	–30	–20	–10
0.27	75	224	210	193	169	119
	40	186	173	156	135	98
0.36	75	245	232	213	187	142
	40	204	191	175	149	111

The nonlinear regressional relationship for the subcool zone length is given by:

$$L_x = -51.54 - 5.17t_{ext} - 0.047t_{ext}^2 + 206.67\left(\frac{S_t}{S}\right) + 1.02v_t. \quad (8)$$

For (8) the criterion $R^2 = 0.99$, the confidence coefficient is 95%, the effective ranges $t_{ext} \in [-50; -10°C]$, $S_t / S \in [0.27; 0.36]$, $v_t \in [40; 75$ km/h]. Relationship (8) shows that the length of the subcool zone depends on the train velocity, train/tunnel cross section overlap ratio, face gate operation and atmospheric air temperature. The subcool span is longer in the tunnel with closable gates I than in the tunnel with open faces (Fig. 3c).

Thus, we have determined the tunnel air temperature patterns in the tunnel from the outlet face depthward the tunnel versus the train travel time and the distance from the tunnel face and the train point inside the tunnel, as well as the dependence of the subcool zone length in the cold season on the outer air temperature, train/tunnel cross section overlap ratio and the train.

2. EFFICIENCY OF METHODS TOWARD ANTI-ICING AND ANTI-FROST DAMAGE OF LINING IN FACE ARES OF TUNNELS

The outlet face in the cold season experiences variable air temperatures during train movement. To prevent lining subcooling down to $t_0 = 0°C$ and below, some methods can be used, such as heating cable, heat insulation of lining and arrangement of cool gallery in the face area.

Self-tuning heating cable. The operation of a self-tuning heating cable consists in the change of electrical resistance and, accordingly, current intensity during heating or cooling of the cable, which allows maintenance of the lining temperature without using external heat controllers. The cable is put at a certain spacing in outer concrete coat of lining. When connected to power, the cable maintains the temperature at the required level. This allows saving of power in lining heating. The heat production of the cable can be adjusted versus the actual air temperature at the lining, train traffic and the actual outer air temperature.

The critical characteristics of a heating cable are the heat power q_l per unit length and the temperature t_k. For finding q_l and t_k as function of the outer air temperature, the heat transfer processes were analyzed within the tunnel length equal to a cable laying length l_k. The geometry and boundary conditions of the heat transfer model are depicted in Fig. 4.

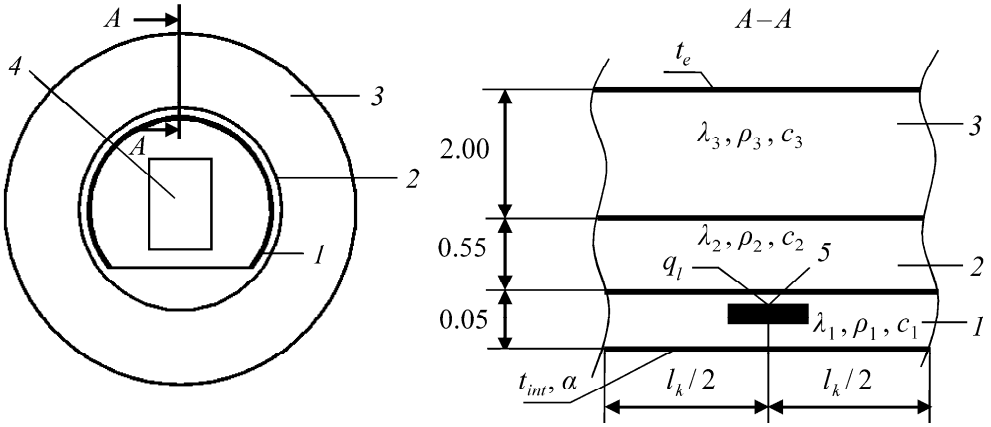

Fig. 4. Geometry and boundary conditions of heat transfer model: *1*—concrete coat; *2*—tubing; *3*—rock mass; *4*—train; *5*—heating cable; t_{int}—tunnel air temperature; α—heat-transfer coefficient from the tunnel lining to the tunnel air; t_e—natural temperature of rock mass; λ_1, ρ_1, c_1, λ_2, ρ_2, c_2, λ_3, ρ_3, c_3—respectively, heat conductivity factor, density and heat capacity of concrete coat (subscript 1), tubing (subscript 2) and rock mass (subscript 3).

The mathematical modeling of heat transfer in the sandwich enclosing structure of a railway tunnel is based on the numerical solution of the initial boundary value problem for the equation of conservation of heat energy [4, 6]:

$$\rho \frac{\partial h}{\partial \tau} = \nabla(\lambda \nabla t) + S_E . \tag{9}$$

The size of the discussed span is small as compared with the radius of the tunnel, and the curvature of this span is neglected therefore. The enclosing structure of the Severmuysky Tunnel is a typical sandwich: *1*—concrete coat with the thickness $\delta_2 = 0.05$ m, $\lambda_1 = 0.58$ W/m, $\rho_1 = 1800$ kg/m^3, $c_1 = 840$ J/(kg°C); *2*—reinforced concrete tubing with the thickness $\delta_2 = 0.55$ m, $\lambda_2 = 1.69$ W/m, $\rho_2 = 2500$ kg/m^3, $c_2 = 840$ J/(kg°C); *3*—enclosing rock mass with the thickness $\delta_3 = 2$ m, $\lambda_3 = 2.4$ W/m, $\rho_3 = 2560$ kg/m^3, $c_3 = 1000$ J/(kg°C) [7]. At the outer boundary of the model, the natural rock mass temperature is set as $t_e = 5$ °C. At the concrete coat and air interface, the temperature was set as t_{int} to vary from 0 to –50°C at an increment of 10°C and the heat-transfer coefficient α of 8.25–19.72 W/(m^2°C). The convective heat transfer between the tunnel air and the lining surface was taken into account in accordance with (7). As we discuss only a part rather than the whole enclosing structure of the tunnel, at the side boundaries we set the periodicity conditions $f(t_{left}) = f(t_{right})$.

The computation experiment produced the values for the heat power q_l and heating cable temperature t_k at the cable laying lengths of 0.1, 0.2 and 0.3 m (Figs. 5a and 5c). The transition from the heating cable power q_l (W/m) to the lining heating power q_F (W/m^2) uses the formula $q_F = q_l / l_k$. The temperature dependence of the lining heat power $q_F(t_{ext})$ is given in Fig. 5b.

The obtained results make it possible to find the cable heat power sufficient to maintain the constant lining temperature not less than 4°C. The general regressional relationship between the lining heat power q_F, cable laying length and the air temperature is given by:

$$q_F = -223.2 l_k + 1539 l_k^{\,2} - 6.24 t_{int} + 0.04 t_{int}^2 . \tag{10}$$

For (1) the criterion $R^2 = 0.99$, the confidence coefficient is 95%, the ranges of application of (10) are $t_{int} \in [-50; 0°C]$, $l_k \in [0.1; 0.3$ m$]$.

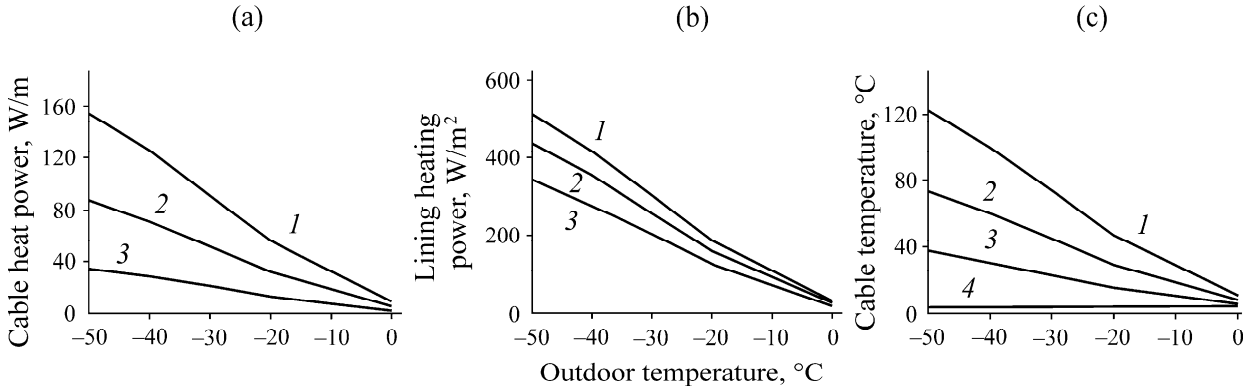

Fig. 5. Heating cable parameters sufficient to maintain lining surface temperature 4°C: (a) cable heat power q_l versus outer air temperature; (b) lining heating power q_F ; (c) cable temperature at cable laying lengths *1*— 0.3; *2*—0.2 and *3*—0.1 m; *4*—required temperature of lining surface is 4°C.

The electric power to hear the tunnel lining at the outlet face is found from the formula:

$$Q_k = q_F P_t L_x, \tag{11}$$

P_t is the perimeter of the tunnel cross section, m.

The choice of a heating cable is an optimization problem with:

$$\begin{cases} t_o \geq t_o^{dem} \\ t_k \to \min \\ q_F \to \min \\ C_k \to \min \end{cases}$$

Here, t_o is the tunnel lining temperature, °C; t_o^{dem} is the demanded lining temperature, °C; t_k is the heating cable temperature, °C; q_F is the heat power to heat the lining, W/m^2; C_k is the cable installation cost, Rub. The heat power of the heating cable is withdrawn from the tunnel heat balance as the heat flow from the lining to the inner air in the tunnel is minimal due to insignificant temperature difference.

Heat insulation of inner surface in tunnels. We discuss a version of heat insulation of tunnel lining inside the subcool zone at the tunnel face. This version is free from the heating power expenses, and the tunnel opening is smaller. For finding the actual temperature on the surface of the tunnel lining versus the heat insulation thickness and the outdoor air temperature, the numerical model is developed to calculate heat transfer processes in the lining structure. The geometry and the boundary conditions of the model are presented in Fig. 6.

The tubing is as in the Severmuysky Tunnel. The heat insulation is made of mineral wool plates with a synthetic binder, with the thermophysical characteristics as follows: $\lambda_4 = 0.038$ W/m, $\rho_4 = 180$ kg/m^3, $c_4 = 840$ J/(kg°C) [7]. The computation results are the temperatures on the lining surface as against the heat insulation thickness δ_{is} and the air temperature t_{int} (Fig. 7).

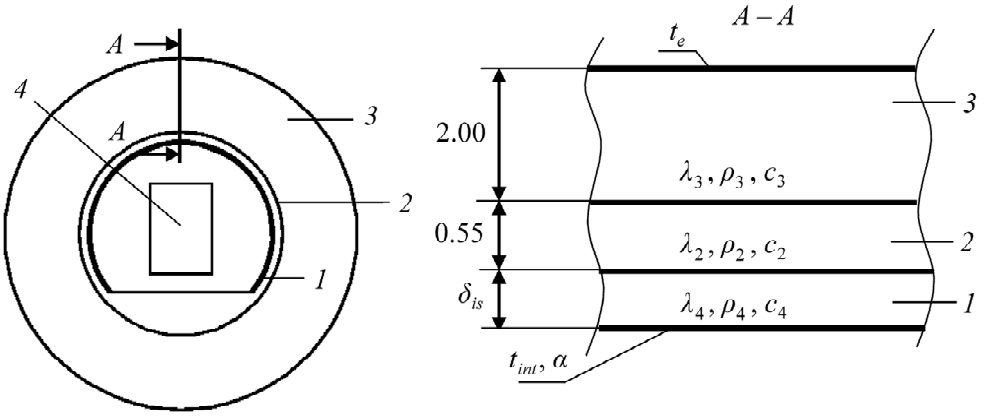

Fig. 6. Geometry and boundary conditions of heat transfer model: *1*—heat insulation layer; *2*—tubing; *3*—enclosing rock mass; *4*—train; t_{int}—tunnel air temperature; α—heat-transfer coefficient from the tunnel lining to the tunnel air; t_e—natural temperature of enclosing rock mass; λ_4, ρ_4, c_4, λ_2, ρ_2, c_2, λ_3, ρ_3, c_3—respectively, heat conductivity factor, density and heat capacity of concrete coat (subscript 1), tubing (subscript 2) and rock mass (subscript 3).

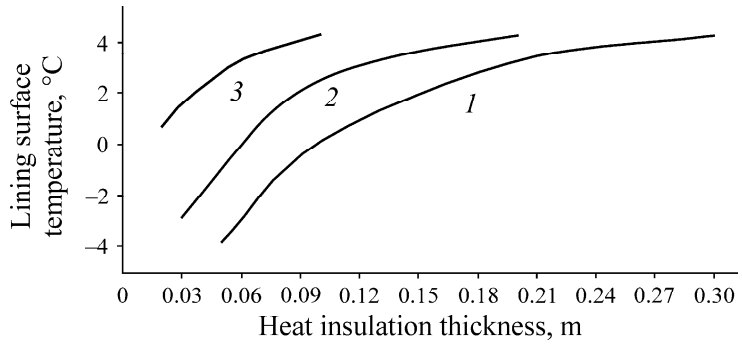

Fig. 7. Temperature of tunnel lining versus heat insulation thickness at outdoor temperatures t_{int} = –50°C (*1*), –30 (*2*) and –10 (*3*).

When the heat insulation layer is thicker than 0.25 m, the required temperature not less than 4°C is achieved at the insulation–tubing interface. The regressional relationship of the lining surface temperature, insulation temperature and outdoor temperature is given by:

$$t_{obd} = 14.8 + 3.57\ln(\delta_{is}) + 0.1368 t_{int}\,.$$

For this relationship, the criterion $R^2 = 0.95$, the confidence coefficient 95%, the application ranges are $t_{int} \in [-50; -10°\text{C}]$, $\delta_{is} \in [0.03; 0.30\ \text{m}]$. A shortage of this method to prevent frost damage of lining is the reduction in the tunnel opening, which can affect operational efficiency.

Cool gallery. A cool gallery arranged in the face area is another method of decreasing heat lost in heating coal air inflow as a train leaves a tunnel. The cool gallery is an extension of the tunnel. The gallery represents a modular structure made of steel or polymeric material unsusceptible to frost damage tightly adjacent to the tunnel face.

The computation model of heat transfer in the cool gallery is depicted in Fig. 8. The idea of the cool gallery is to arrange a next-to-outlet face span to be exposed to negative temperatures of cold outdoor air which cannon get to the tunnel lining therefore. Train *2* goes through outlet *7* from gallery *5* and outdoor air with temperature t_{ext} is drawn the gallery (Fig. 8). The gallery is free from wet and subcooling down to negative temperature results in no icing and frost damage of the gallery walls. As the train goes out of the gallery, in the time period between trains, the gallery is filled with warm air with the temperature t_{int} flowing in the line from 3 to *6* in Fig. 8.

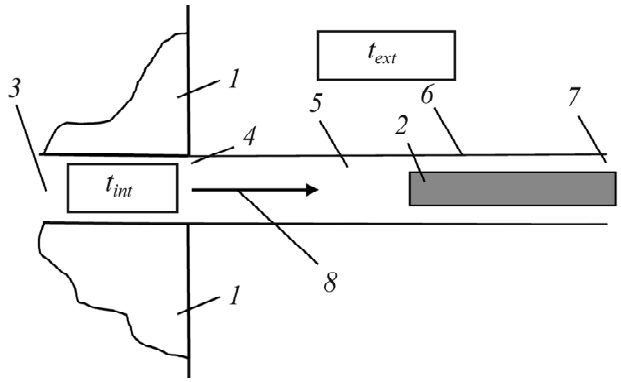

Fig. 8. Face gallery: *1*—enclosing rock mass around tunnel; *2*—outgoing train; *3*—tunnel; *4*—tunnel outlet; *5*—gallery; *6*—gallery walls; *7*—gallery outlet; *8*—air flow direction in gallery; t_{ext}—outdoor air temperature; t_{int}—tunnel air temperature.

We assessed variation in air temperature along a cool gallery with the length $l_g = 500$ m depending on the air velocity using the Severmuysky Tunnel as a model and two alternatives of the gallery enclosure:

—unwinterized gallery made of sheet metal with $\delta_g = 0.005$ m;

—winterized gallery with a mineral wool layer ($\lambda_{i,g} = 0.038$ W/(m°C), $\rho_{i,g} = 180$ kg/m^3, $c_{i,g} = 840$ J/(kg°C), $\delta_{i,g} = 0.1$ m).

In standard mode of operation, air with the temperature $t_{int} = 4\,°\text{C}$ flows from the tunnel in the gallery, fills it and goes out from the open end of the gallery. The warm air velocity depends on the operating mode of the tunnel, i.e., on the position of the face gates (open or shut) and on the time period between trains.

Using the methods of static air distribution, we obtain the representative air velocities in the tunnel:

- $v_{int} = 3.70$ m/s—maximal air velocity at train frequency of 6 train per hour at the train-to-train interval of 10 min, when the tunnel gates are open and one train moves out of the tunnel and another train simultaneously enters the tunnel at the maximal running speed of 75 km/h;
- $v_{int} = 1.78$ m/s—average air velocity in the interval between trains, with open gates in the tunnel, the train-to-train interval is less than 10 min;
- $v_{int} = 0.60$ m/s—minimal air velocity (owing to leaks through the face gates) when trains move in the tunnel with closed gates of the faces and with the train-to-train interval of 20 min and longer.

The distance covered by warm air flow within the time τ between trains is: $l_{air} = 2220$ m at $v_{int} = 3.70$ m/s; $l_{air} = v\tau = 1068$ m at $v_{int} = 1.78$ m/s and $l_{air} = 720$ m at $v_{int} = 0.60$ m/s. At such velocities warm air fills the gallery completely within the time interval between trains.

The variation in the tunnel air temperature is studied for $v_{int} = 4°\text{C}$, $t_{ext} = -45°\text{C}$, and air velocities of 0.60, 1.78 and 3.70 m/s using 2D axially symmetric models by the methods of computational aerodynamics and heat transfer in the software environment ANSYS Fluent. Equations (1)–(3) are solved using the RNG $k-\varepsilon$ model:

$$\frac{\partial}{\partial \tau}(\rho k) + \frac{\partial}{\partial x_i}(u_i k \rho) = \frac{\partial}{\partial x_j}\left(\alpha_k \mu_{eff} \frac{\partial k}{\partial x_j}\right) + G_k + G_b - \rho\varepsilon - Y_M + S_k, \tag{12}$$

$$\frac{\partial}{\partial \tau}(\varepsilon\rho) + \frac{\partial}{\partial x_i}(u_i \varepsilon \rho) = \frac{\partial}{\partial x_j}\left(\alpha_k \mu_{eff} \frac{\partial \varepsilon}{\partial x_j}\right) + C_{1\varepsilon}\frac{\varepsilon}{k}(G_k + C_{3\varepsilon}G_b) - C_{2\varepsilon}\rho\frac{\varepsilon^2}{k} - R_\varepsilon + S_\varepsilon, \tag{13}$$

$$d\left(\frac{\rho^2 k}{\sqrt{\varepsilon\mu}}\right) = 1.72\frac{\hat{\nu}}{\sqrt{\hat{\nu}^3 - 1 + C_\nu}}d\hat{\nu}, \tag{14}$$

$$\hat{\nu} = \frac{\mu_{eff}}{\mu}, \tag{15}$$

$$C_\nu \approx 100. \tag{16}$$

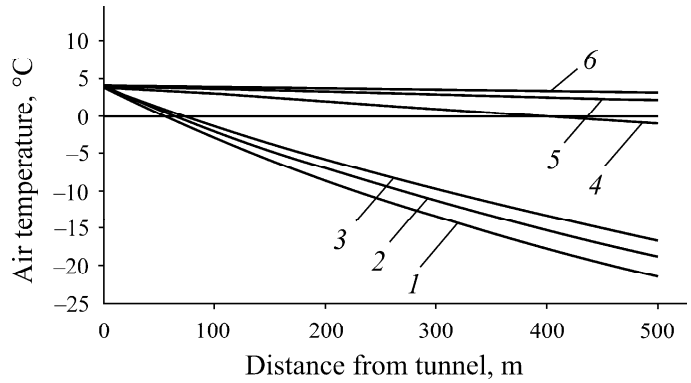

Fig. 9. Change in tunnel air temperature in flowing in gallery at velocities, m/s: *1*—0.60; *2*—1.78; *3*—3.70; *4*—0.60 with heat insulation; *5*—1.78 with heat insulation; *6*—3.70 with heat insulation; 0 m—outlet from tunnel to gallery; 500 m—outlet from gallery outwards.

In expressions (12)–(16), u_i is the vector field of velocities; ε is the dissipative turbulent kinetic energy, J/(kg·s); μ_{eff} is the effective dynamic viscosity, Pa·s; $C_{1\varepsilon} = 1.42$, $C_{2\varepsilon} = 1.68$, $C_\nu = 100$, $\alpha_k = 1.193$ are the constants of the turbulence model; G_k, G_b, Y_M, S_k, $C_{3\varepsilon}$, R_ε, S_ε are the values found from solutions of additional equations [4]. The calculated averaged air temperatures t_g across the gallery section are given in Fig. 9 and Table 2.

In an unwinterzied gallery, the minimal air temperature when air flows in the tunnel as a train leaves it is –21.4°C at the outdoor air temperature $t_{ext} = -45$°C, which allows the decrease in the heat capacity of the air door at the face by 48.2%. In a winterized gallery with the heat-insulated walls, air flow into the tunnel has a positive temperature in the same conditions, which eliminates heat expenses connected with heating air inflow from the outside when a train leaves the tunnel. Cold outdoor air cannon reach the tunnel, which prevents icing and frost damage of the tunnel lining.

The cool gallery is an effective method to combat frost damage of lining in tunnels. On the other hand, given no damp proofing in the tunnel, the gallery undergoes icing owing to moisture condensation after cooling of moist tunnel air. To prevent icing in the cool gallery, it is required to install heat insulation and a heating cable within a span to 100 m long from the outlet from the gallery (Fig. 9).

Table 2. Average air temperature in various cross sections longwise the gallery, t_g °C

Distance from the tunnel outlet, m	Air velocity v_{int}, m/s					
	With heat insulation			Without heat insulation		
	0.60	1.78	3.70	0.60	1.78	3.70
1	4.0	4.0	4.0	3.7	3.8	3.8
125	2.7	3.5	3.8	–4.5	–3.4	–2.6
250	1.4	3.0	3.5	–11.1	–9.2	–7.9
375	0.2	2.6	3.3	–16.8	–14.4	–12.6
500	–1.0	2.1	3.0	–21.4	–18.8	–16.7
Average	1.5	3.0	3.5	–10.0	–8.4	–7.2

3. AIR TEMPERATURE IN TUNNEL IN THE COLD SEASON

Variation patterns of air temperature lengthwise tunnels operating in Russian Siberia and Far East are understudied so far, which affects the quality of thermal condition design for tunnels and impairs correct selection of heating fan installations. The current literature on ventilation in long traffic tunnels mostly focus on the influence exerted by the piston effect and radiation pollution on ventilation performance in tunnels [8–17]. Some studies address heat transfer processes in underground excavations, their cooling and artificial freezing [18–20]. However, the test subject—temperature fields in surrounding rock mass around mines—is so specific and the results cannot be applied to aerothermodynamic processes in traffic tunnels.

The analysis of the heat balance components in a tunnel, in particular, loss of heat in warming a train in [21] left the air temperature variation along the tunnel aside. The studies into the actual; air temperatures in the Severomuysky Tunnel [22] reveals that at outdoor temperature of –25 – –35°C the tunnel air temperature fluctuates at 0°C, while the theoretical temperature recommended for the ventilation system design for tunnels is –40°C [23]. The location and prospects for convertible aircraft turbojet engines are justified without any studies into air temperature variation along tunnels [24–26]. The radial distribution of temperature in enclosing rock mass and per cross sections is analyzed in a case-study of the Nanshan Tunnel in Qinling, China [27]. This region features wet moderate continental–monsoon climate with a long, cold and snowy winter and a cool most summer. The lowest regional temperature is –17°C, which makes it impossible to apply the research findings to the Baikal–Amur Mainline tunnels. The temperature conditions in enclosing rocks with high temperature are analyzed in [28], and the piston effect and dust distribution in tunnels are studied in [29, 30]. A series of studies into thermal conditions in tunnels and shallow subways give details of variation patterns of temperature in the surrounding rock mass and comprehensively describe heat flow through enclosures [14, 31–33] but the temperature variation patterns determined for subway tunnels are inapplicable directly to the structure and operating conditions of railway tunnels.

The temperature behavior analysis in a railway tunnel versus location of fan heaters can help predict unfavorable areas either with negative air temperature or with excessive heat in the tunnel. The respective research is performed as a case-study of the Severomuysky Tunnel with gates open at one end and shut at the other end. The train/tunnel cross section overlap ratio $S_t / S = 0.27$, the tunnel length is 15357 m, the traffic is maximal, or 6 train per hour with a train-to-train interval of 10 min, the train velocity is 75 km/h and the freight trains are composed of 71 cars. The mathematical model of heat transfer is undertaken for single-side forward and single-side back travels of trains. The calculation procedure is based on dividing the tunnel into some segments and on the air temperature determination at their boundaries. The computational model of an *i*-th segment of the tunnel is depicted in Fig. 10.

The average hourly temperature at the end of the tunnel is calculated from the formula:

$$t_i^{end} = t_i^{beg} + \frac{Q^{i,+} - Q^{i,-}}{c\rho_i L}.$$

Here, t_i^{beg} is the initial temperature in the segment i, °C; $Q^{i,+}$, $Q^{i,-}$ are the heat input and heat loss in the segment i, W [19]; $c = 1005$ is the air heat capacity, J/(kg·°C); ρ_i is the average air density in the segment, kg/m^3; L is the air flow rate in the tunnel, m^3/s. The value of L is constant in all segments; the air flow rate in the tunnel with open ends and with closable gates is determined in [18].

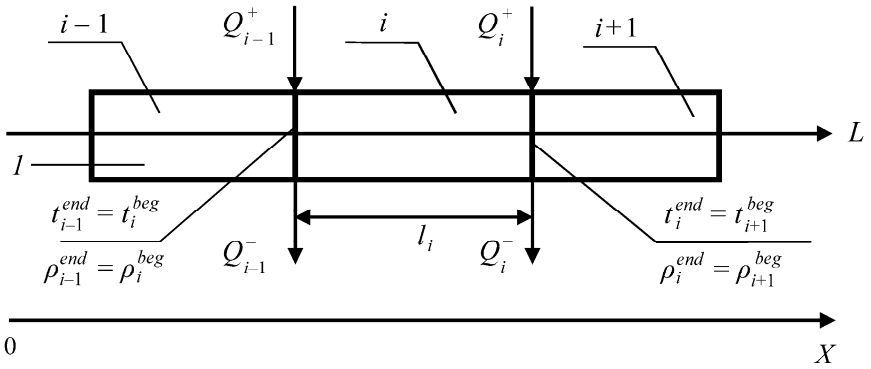

Fig. 10. Computational model of an *i*-th segment in tunnel: $i-1$, i, $i+1$—numbers of segments; L—air flow rate in tunnel; t^{beg}, t^{end}—initial and final air temperatures in the segment, °C; ρ^{beg}, ρ^{end}— initial and final air densities at the beginning in the segment, kg/m^3; l_i—length of the segment, m; Q^+, Q^-—average heat input (from fan heaters) and hourly heat loss (from cold train walls, warming of air at inlet and outlet) in the segment, W; *1*—tunnel; axis $0X$ shows the direction of step-by-step calculation.

The model includes some assumptions: the uniform heat losses lengthwise the tunnel are summed up and are reduced at the end of a segment; the average air density in the segment i is calculated using the air temperatures determined in the segment $i-1$; the heat loss in warming of train, calculated in [15], are adjusted using the relation:

$$Q^{i,-}_{tr,act} = Q^{i,-}_{tr} \frac{t^{beg}_{tr,i} - t^{beg}_i}{\Delta t_0},$$

Δt_0 is the temperature difference between the train wall and the tunnel air; the values of $Q^{N,-}_{tr}$ for it are found in [19].

The train temperature at the beginning of a theoretical segment $N\, t^{beg}_{tr,N}$ is given by:

$$t^{beg}_{tr,i} = t^{end}_{tr,i-1} = t^{beg}_{tr,i-1} + \varphi \frac{(t^{beg}_{tr,i-1} - t^{end}_{i-1})\, l_i}{v_{tr}},$$

where $t^{end}_{tr,i-1}$, $t^{beg}_{tr,i}$, $t^{beg}_{tr,i-1}$ are, respectively, the final temperature of the train wall in the previous segment, and the initial temperatures of the train wall in the current and previous segments, °C; t^{end}_{i-1} is the final air temperature in the previous segment, °C; v_{tr} is the train velocity in the segment, m/s; $\varphi = 0.000237$ 1/s is the proportionality factor to characterize variation in the tunnel air temperature along the segment.

In the segment $i = 1$, the temperature $t^{beg}_{tr,i}$ is equal to the theoretical outdoor temperature t_{ext}. The final air temperature t^{end}_i in the segment i is the initial air temperature t^{beg}_i in the segment $i+1$. The initial air temperature in the first segment at the inlet face of the tunnel is assumed to be equal to the outdoor temperature $t^{beg}_i = t_{ext} = -40$°C. The calculation proceeds gradually from segment to segment in the direction of the train movement in the tunnel at different locations and number of fan heaters.

Figure 11 demonstrates some arrangements of fan heaters in the tunnel.

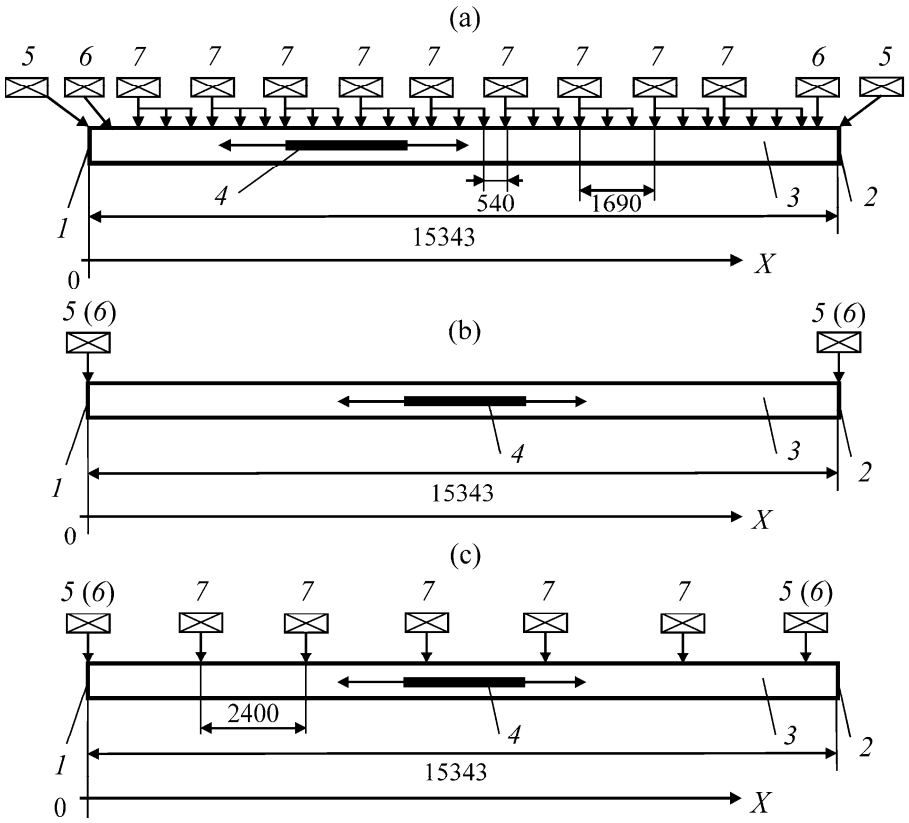

Fig. 11. Arrangements of fan heaters in tunnel: (a) warm air curtains at tunnel faces, integrated in the longitudinal–transverse ventilation system (for one-way traffic); (b) fan heaters at tunnel inlet and outlet; (c) uniform distribution of heat capacity of fan heaters at equal pitches along the tunnel; *1*—inlet; *2*—outlet; *3*—tunnel; *4*—train; *5*—fan heater at inlet; *6*—fan heater at inlet and outlet; *7*—local fan heaters.

In the three schemes, the total heat capacity of fan heaters is the same and equals 13.095 MW [21], equal to the heat loss in the tunnel, i.e. there is a heat balance. Scheme (a) in Fig. 11 shows the warm air curtains installed at the tunnel faces and integrated in the longitudinal–transverse ventilation and air heating in the tunnel. The distance between the warm air escape facilities is determined as the length of way of heated air flow at the velocity v_{int} during the time period between trains. In scheme (b) all heating capacity is concentrated at the tunnel faces and is emanated by the war air curtains. The tunnel is free from extra fan heaters. In scheme (c) the fan heaters with mostly equal heat capacities are placed at the same spacing (2400 m) along the tunnel, which is longer than the way covered by the heated air flow at the velocity v_{int} during the time period between trains. For schemes (a)–(c) in Fig. 11, we analyze operation with one-way and two-way (reverse) traffic of trains.

The research data on the internal air temperature $t_{int} = t_i^{end}$ along the tunnel and the moving train temperature $t_{tr,i}^{beg}$ at the outdoor temperature $t_{ext} = -40°C$ are presented in Fig. 12. In scheme (a) from Fig. 11, the tunnel air is uniformly heated at the extreme temperatures up to 32–36 °C at the tunnel outlet (Fig. 12a). This is connected with the operation of the war curtain meant for heating cool air inflow when the train leaves the tunnel though the outlet face. In schemes (b) and (c) in Fig. 11, no uniform heating of the tunnel interior is achieved:

- in scheme (b) in Fig. 11, in reverse movement of trains, the face areas of the tunnel are overheated while negative temperature zones are observed in the pan 6 km long in the middle of the tunnel; in one-way traffic, starting from 4800 m from the inlet face and up to the outlet face, the inner air temperature in the tunnel have negative values to –30°C (Fig. 12b);

• in reverse movement scheme (c) in Fig. 11, air is underheated at the tunnel faces while overheat zones with the air temperature to 30°C are observed in the span 5 k long in the middle of the tunnel; in one-way traffic, in the span 5400 m long from the inlet face, the air temperature is mostly negative in the tunnel; in the span with the length of 5400 m to the outlet, the air is heated to the temperature up to 60°C, which is essentially higher than the standard (Fig. 12c).

For finding the best arrangement of heating and ventilating facilities based on the wanted temperature maintenance in the tunnel, we introduce the criterion of energy perfection of heating and ventilation:

$$K = K_1 \left| K_2 \right|. \tag{17}$$

The members of (17) are determined as follows:

$$K_1 = \begin{matrix} -1 \text{ if } t_{int}^{\min} < 0, \\ +1 \text{ if } t_{int}^{\min} \geq 0, \end{matrix} \quad K_2 = \frac{1}{L t_{int}^{dem}} \int_0^L t_{int}(l) dl,$$

where $t_{int}^{\min}$ is the minimal air temperature in the tunnel, °C; t_{int} is the air temperature in the calculation segment; t_{int}^{dem} is the required air temperature in the tunnel (4°C); l, L is the length of the segment and tunnel; $t_{int}(l)$ is the tunnel air temperature as function of the tunnel length.

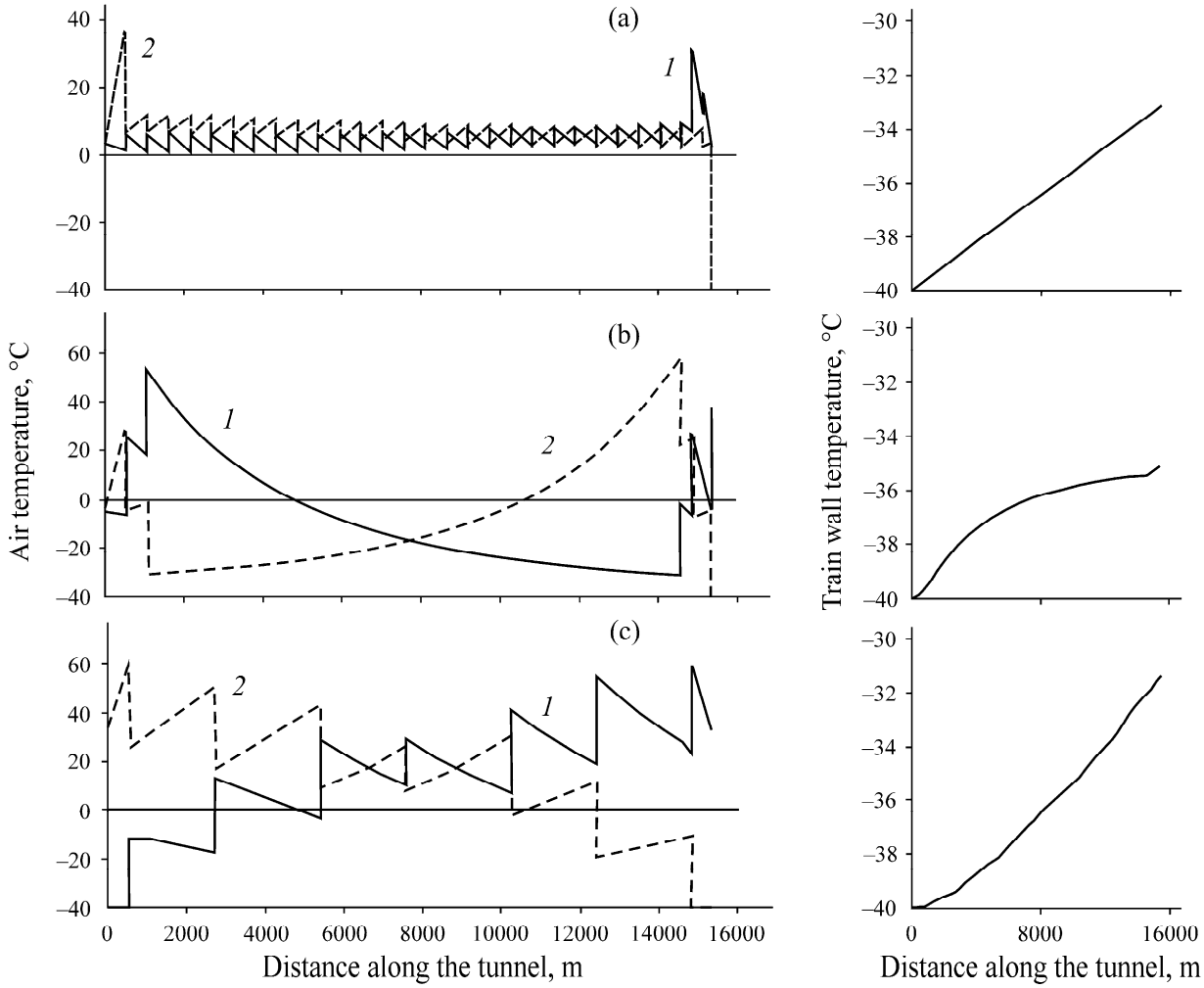

Fig. 12. Tunnel air temperature (left) and train wall temperature (right) in schemes (a)–(c) of train traffic in tunnel; *1*, *2*—forward and reverse motion.

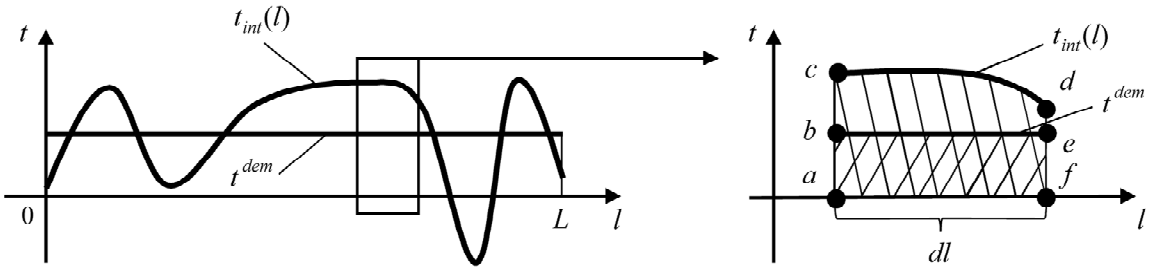

Fig. 13. Finding coefficient K_2.

Table 3. Energy perfection criteria for different schemes of tunnel heating and ventilation (Fig. 11)

Criterion	Scheme (a)	Scheme (b)	Scheme (c)
K_1	1.00	–1.00	–1.00
K_2	1.24	–1.80	3.69
K	1.24	–1.80	–3.69

The coefficient K_1 in formula (17) proves the validity of the heating and ventilating system. If K_1 is negative, the system is incapable to maintain the positive air temperature in the tunnel and is therefore inapplicable. The coefficient K_2 is a ratio of actual energy spent for air heating in the tunnel to the required energy to maintain the tunnel air temperature at t_{int}^0. Geometrically, this is the ratio of areas *abcdef* and *abef* in the test segment of the tunnel (Fig. 13). Ideally, the coefficient K should equal 1. This means that the wanted positive temperature is maintained along the entire tunnel and the heat expenses connected with air heating in the tunnel conform with the set air loss, i.e. there is a balance of heat loss and heat input in the tunnel.

The coefficients K_1, K_2 and K for schemes (a)–(c) in Fig. 11 are given in Table 3. Scheme (a) has the criterion nearest to one. Schemes (b) and (c) are inapplicable to heating and ventilating tunnels as:

—in scheme (b) the coefficients K_1 and K_2 are negative; there are areas with negative air temperatures, and actual energy spent for heating is less than the standard;

—in scheme (c) the coefficient K_1 is negative; there are areas with negative air temperatures in the tunnel.

CONCLUSIONS

The extension of the subcool zone in the tunnel lining depthward the tunnel from its outlet, which appears when a train leaves the tunnel, is determined versus the inner air temperature in the tunnel, the outdoor air temperature, the train/tunnel cross section overlap ratio and the train velocity. The methods to prevent icing in the tunnel are discussed, and the engineering and design parameters of the tunnel are substantiated.

In a one-track tunnel for forward and reverse movement of trains, it is found how the inner air temperature in the tunnel in the cold season depends on the layout of fan heaters in the tunnel. The proposed criterion of energy perfection of the heating and ventilating systems helps estimate efficiency of a chosen layout of fan heaters. It is found that the scheme with all heating capacities arranged at the tunnel faces and the scheme with fan heaters installed at equal spacing lengthwise the

tunnel fail to maintain the positive air temperature in the tunnel. The most effective scheme is combination of the warm air curtains set at the tunnel faces with fan heaters installed uniformly along the tunnel at spacing equal to the length of way covered by war air flow between the neighbor fan heaters in the period when there are no trains in the tunnel.

REFERENCES

1. Lugin, I.V. and Vitchenko, A.A., Maintaining Required Temperature Conditions in the Severomuysky Tunnel in Cold Season Using the Tunnel Ventilation Facilities, *J. Fundament. Appl. Min. Sci.*, 2014, vol. 1, no. 1, pp. 210–214.
2. Gendler, S.G., Basic Trends in Modernization of Ventilation System in the Baikal Railway Tunnel, *GIAB*, 2013, Special Issue 1, pp. 288–296.
3. *Construction Regulations SP 122.13330.2012*, Railway and Road Tunnels, Moscow, 2012.
4. *Ansys User's Help Viewer*, Version 2019 R3.
5. Baturin, O.V., Baturin, N.V., and Matveev, V.N., *Raschet techenii zhidkostei i gazov s pomoshch'yu universal'nogo programmnogo kompleksa Fluent* (Calculation of Fluid Flows Using Universal Software Fluent), Samara: SamGU 2009.
6. Fedorova, N.N., Val'ger, S.A., Danilov, M.N., and Zakharova, Yu.V., *Osnovy raboty v ANSYS 17* (Backbone of Operations in ANSYS 17), Moscow: DMK Press, 2017.
7. *Construction Regulations SP 50.13330.2.12*, Heat Protection of Buildings, Moscow, 2013.
8. Gendler, S.G. and Pleskunov, V.A., Efficient Ventilation Design for the Kuznetsovsky Railway Tunnel, *GIAB*, Special Issue 13, 2009, pp. 81–89.
9. Gendler, S.G., Kastaneda, V.A., and Belen, A.G., Control of Natural Air Flow in Road Tunnels, *Mining Informational and Analytical Bulletin—GIAB*, 2012, no. 4, pp. 138–149.
10. Gendler, S.G., Smirnyakov, V.V., and Sokolov, V.A., Early In-Situ Test Data on Ventilation System in the Severomuysky Railway Tunnel, *GIAB*, 2005, Special Issue 2, pp. 272–281.
11. Gendler, S.G. and Mironenkova, N.A., Efficient Ventilation Design for Railway Tunnels in Harsh Climate Regions by the Radiation Criterion, *GIAB*, 2008, Special Issue 5, pp. 298–306.
12. Gendler, S.G. and Savenkov, E.A., The Use of Jet Fans in Ventilation of Railway Tunnels, *GIAB*, 2015, Special Issue 7, pp. 26–31.
13. *DIN EN 14067*. Bahnanwendungen. Aerodynamik. Teil 3: Aerodynamik im Tunnel. Deutsche fassung EN 14067-3, 2003.
14. Krasyuk, A.M., Lugin, I.V., and Pavlov, S.A., Experimental Research into Air Distribution in a Terminal Subway Station, *Tunneling and Underground Space Technol*., 2019, vol. 85, pp. 21–28.
15. Krasyuk, A.M., Lugin, I.V., Alferova, E.L., and Kiyanitsa, L.A., Evaluation of Ventilation Flow Charts for Double-Line Subway Tunnels without Air Chambers, *Journal of Mining Science*, 2016, vol. 52, no. 4, pp. 740–751.
16. Yueming Wen, Jiawei Leng, Xiaobing Shen, Gang Han, Lijun Sun, and Fei Yu, Environmental and Health Effects of Ventilation in Subway Stations: A Literature Review, *Int. J. of Environmental Res. and Public Health*, 2020, vol. 1084, no. 117, P. 37.
17. Yueming Wen, Jiawei Leng, Fei Yu, and Chuck Wah Yu, Integrated Design for Underground Space Environment Control of Subway Stations with Atriums Using Piston Ventilation, *Indoor and Built Environment*, 2020, Vol. 16, No. 1.
18. Semin, M.A., Levin, L.Yu., Zhelnin, M.S., and Plekhov, O.A., Natural Convection in Water-Saturated Rock Mass under Artificial Freezing, *Journal of Mining Science*, 2020, vol. 56, no. 2, pp. 297–308.

19. Levin, L.Yu., Semin, M.A., and Zaitsev, A.V., Adjustment of Thermophysical Rock Mass Properties in Modeling Frozen Wall Formation in Mine Shafts under Construction, *Journal of Mining Science*, 2019, vol. 55, no. 1, pp. 157–168.
20. Kaimonov, M.V. and Khokholov, Yu.A., Selection of Frozen Backfill Mixture Composition, *Journal of Mining Science*, 2019, vol. 55, no. 5, pp. 857–864.
21. Lugin, I.V. and Alferova, E.L., Heat Losses during Train Movement in an Underground Tunnel under Various Operating Conditions , *J. Fundament. Appl. Min. Sci.*, 2019, vol. 6, no. 2, pp. 181–185.
22. Gendler, S.G. and Belov, M.R., Basic Trend in Improvement in Heating and Ventilating System in the Severomuysky Tunnel for Heavier Traffic, *GIAB*, 2019, Special Issue 4/6, pp. 45–57.
23. *Construction Regulations SP 131.13330.2018*, Climatology in Construction, Moscow, 2019.
24. Krasyuk, A.M., Lugin, I.V., and Kulikova, O.A., Application of Turbojet Two-Circuit Engine for Sustained Thermal Environment in Railway Tunnels in Severe Climatic Conditions, *Mining Informational and Analytical Bulletin—GIAB*, 2018, no. 2, pp. 103–110.
25. Postnikov, A.M., *Snizhenie oksida azota v vykhlopnykh gazakh GTU* (Reduction of Nitrogen Oxide Content in Exhaust Gas of Gas-Turbine Plant), Samara: SNTS RAN, 2002.
26. Gritsenko, E.A., Danil'chenko, V.P., Lukachev, S.V., Reznik, V.E., and Tsybizov, Yu.I., *Konvertirovanie aviatsionnykh GTD v gazoturbinnye ustanovki nazemnogo primeneniya* (Conversion of Aircraft Gas-Turbine Engines into Gas-Turbine Plants for Ground Application), Samara: SNTS RAN, 2004.
27. Xiaohan Zhou, Yanhua Zeng, and Lei Fan, Temperature Field Analysis of a Cold-Region Railway Tunnel Considering Mechanical and Train-Induced Ventilation Effect, *Applied Thermal Eng*., 2016, vol. 100, pp. 114–124.
28. Yanhua Zeng, Liangliang Tao, Xuqian Ye, Xiaohan Zhoub, Yong Fanga, Lei Fan, Xinrong Liu, and Zongxian Yang, Temperature Reduction for Extra-Long Railway Tunnel with High Geotemperature by Longitudinal Ventilation, *Tunneling and Underground Space Technol*., 2020, vol. 99, P. 16.
29. Jiqiang Niu, Yang Sui, Qiujun Yu, Xiaoling Cao, and Yanping Yuan, Aerodynamics of Railway Train/Tunnel System: A Review of Recent Research, *Energy and Built Environment*, 2020, vol. 1, issue 4, pp. 351–375.
30. Wenjie Zhou, Wen Nie, Xiaofei Liu, Cunhou Wei, Changqi Liu, Qiang Liu, and Shuai Yin, Optimization of Dust Removal Performance of Ventilation System in Tunnel Constructed Using Shield Tunneling Machine, *Building and Environment*, 2020, vol. 173, P. 56.
31. Krasyuk, A.M., Lugin, I.V., and P'yankova, A.Yu., Delineation of Soil Body Area Exposed to Thermal Effect of Subway Stations and Tunnels, *Journal of Mining Science*, 2015, vol. 51, no. 1, pp. 138–143.
32. Krasyuk, A.M., Lugin, I.V., and P'yankova, A.Yu., Temperature Fields in Surrounding Ground of Shallow Tube Stations, *Journal of Mining Science*, 2012, vol. 48, no. 3, pp. 465–473.
33. Kiyanitsa, L.A., Determining Analytical Dependences for Heat Flow in Soil fro, Enclosed Type Shallow Underground Subway Stations with Double-Track Tunnels, *Mining Informational and Analytical Bulletin—GIAB*, 2018, no. 2, pp. 89–102.